Cryobiology 72 (2016) 216–224

Contents lists available at ScienceDirect

Cryobiology

journal homepage: www.elsevier.com/locate/ycryo

A first test of the hypothesis of biogenic magnetite-based heterogeneous ice-crystal nucleation in cryopreservation

Atsuko Kobayashi [a, *], Harry N. Golash [b], Joseph L. Kirschvink [a, c]

[a] Earth-Life Science Institute, Tokyo Institute of Technology, Meguro, Tokyo 152-8551, Japan
[b] Division of Mechanical Engineering, California Institute of Technology, Pasadena, CA 91125, USA
[c] Division of Geological and Planetary Sciences, California Institute of Technology, Pasadena, CA 91125, USA

ARTICLE INFO

Article history:
Received 13 January 2016
Received in revised form
5 April 2016
Accepted 10 April 2016
Available online 14 April 2016

Keywords:
Ice crystal nucleation
Supercooling
Biogenic magnetite
SQUID magnetometry

ABSTRACT

An outstanding biophysical puzzle is focused on the apparent ability of weak, extremely low-frequency oscillating magnetic fields to enhance cryopreservation of many biological tissues. A recent theory holds that these weak magnetic fields could be inhibiting ice-crystal nucleation on the nanocrystals of biological magnetite (Fe_3O_4, an inverse cubic spinel) that are present in many plant and animal tissues by causing them to oscillate. In this theory, magnetically-induced mechanical oscillations disrupt the ability of water molecules to nucleate on the surface of the magnetite nanocrystals. However, the ability of the magnetite crystal lattice to serve as a template for heterogeneous ice crystal nucleation is as yet unknown, particularly for particles in the 10–100 nm size range. Here we report that the addition of trace-amounts of finely-dispersed magnetite into ultrapure water samples reduces strongly the incidence of supercooling, as measured in experiments conducted using a controlled freezing apparatus with multiple thermocouples. SQUID magnetometry was used to quantify nanogram levels of magnetite in the water samples. We also report a relationship between the volume change of ice, and the degree of supercooling, that may indicate lower degassing during the crystallization of supercooled water. In addition to supporting the role of ice-crystal nucleation by biogenic magnetite in many tissues, magnetite nanocrystals could provide inexpensive, non-toxic, and non-pathogenic ice nucleating agents needed in a variety of industrial processes, as well as influencing the dynamics of ice crystal nucleation in many natural environments.

1. Introduction

An ability to freeze biological tissues without causing ultrastructural damage has been a concern of the Electron Microscopy (EM) community for many years. Extensive work by transmission and scanning (TEM/SEM) electron microscopists has shown that freezing rates of ~10,000 °C/s are needed to prevent cellular damage [6], and this can only be achieved for very thin tissue layers at atmospheric pressure. Using high-pressure techniques that move a sample at room temperature into the ice-stability field, followed by cooling, still only allows a tissue thickness of up to 0.6 mm to be processed.

Conversion of a liquid to a solid during freezing requires structural ordering at the molecular level, which is often inhibited unless seed nuclei or epitaxial surfaces are present to help initiate the crystallization process. Retention of the liquid state at temperatures below the melting point is called *supercooling*, and is a dynamically unstable state in many liquids due to the chance probability of an initial seed crystal nucleating. The rapid cooling techniques for thin samples noted above work by forcing the water to supercool faster than damaging ice crystals are able to nucleate. Supercooling is actually a general phenomenon: standardized tables of physical properties of various compounds will list the melting temperature of a substance, rather than its freezing temperature. Melting is the disruption of a pre-existing, ordered atomic lattice, which occurs when the thermal background energy is high enough to disrupt the atomic ordering of a crystal lattice; this happens at temperatures that are far more reproducible than the 'freezing' temperature.

Supercooling is easily achieved in purified bottled water that has been packaged in amorphous PET [polyethylene terephtalate] bottles, and makes for many impressive video demonstrations that are available on-line. Molecular dynamic studies of the

* Corresponding author.
E-mail address: kobayashi.a.an@m.titech.ac.jp (A. Kobayashi).

http://dx.doi.org/10.1016/j.cryobiol.2016.04.003

crystallization of ice-I_h (hexagonal ice polymorph I) suggest that upwards of 250–300 discrete water molecules need to assume a transient long-range ordering in the supercooled state in order to initiate crystal nucleation [35]. Once this low-probability, stochastic nucleation is initiated anywhere in the container, it will spread rapidly until the large latent heat of crystallization of water (~80 calories/g) brings the bulk temperature of the crystallizing mush back up to the melting temperature (0 °C), producing a characteristic step function in the time-temperature profile of supercooled water; an example is shown here in Fig. 1A. Subsequent cooling has little additional effect on the temperature curve, until most of the liquid water that has buffered the material at the freezing point has been incorporated into the growing volume of ice. In contrast, water that contains particles capable of rapidly nucleating ice crystals will not show a pronounced supercooling effect, resulting in more conventional cooling curves like those shown in Fig. 1 B & C.

In nature, ice crystals are thought to nucleate on small dust particles made of a variety of common mineral types that are distributed by æolian and fluvial processes, and are present in most natural freshwater and marine bodies of water, as well as forming the dominant aerosol component in the atmosphere. Most of the research has been focused on common minerals found in æolian dust, as well as condensed organic materials. On the other hand, Atkinson et al. [1] have found that the potassium-rich feldspars provide better ice nucleation sites than the other minerals. In any event, mineral dusts that serve as ice nucleation particles may play a significant role in the dynamics of atmospheric convection and radiation, particularly in view of the large latent heat of crystallization.

With these properties in mind, it is important to mention that ice damage to animal and plant membranes during intracellular freezing is a major obstacle to the use of cryopreservation. The damage is two-fold: the ~10% expansion as water freezes changes

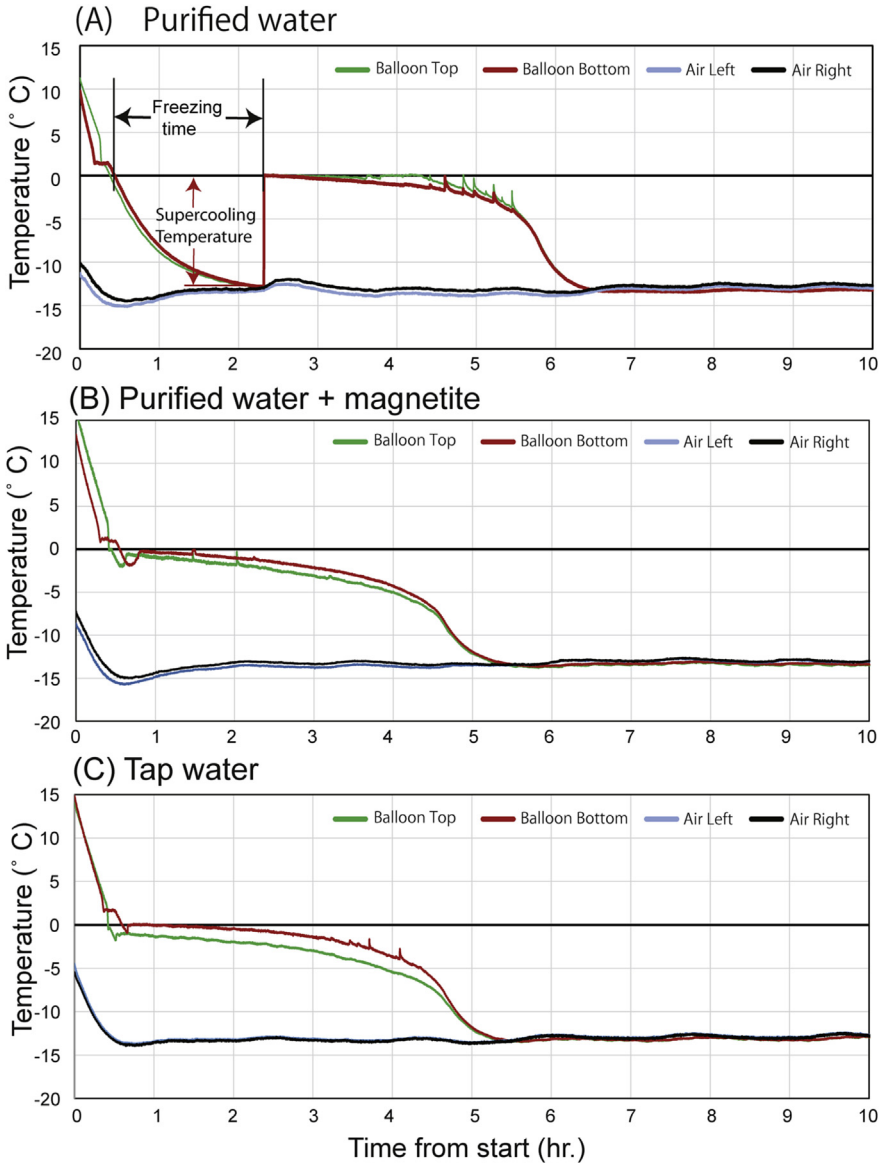

Fig. 1. Examples of time-temperature curves for standard balloon samples, as monitored by the thermocouples placed near the top and bottom of the balloons, and at two points in the cooling chamber. A. Typical example of purified water showing supercooling. Labels show how and where the freezing times and lowest supercooling temperatures were measured from the bottom sensor data, as entered in Table 1. B. Typical example of purified water spiked with ~70 ng/g of standard magnetite powder. C. Cooling curve of laboratory tap water.

the relative volume ratio of membranes to cytosol, potentially disrupting the cytoskeleton and cellular membranes, and, if the crystallization process is slow, needle-like ice crystals can form that can puncture holes in cell membranes as they grow. However, it is a puzzle as to how such intracellular ice crystals actually nucleate – most cellular materials are composed of long polymers (DNA, fatty acids, protein α-helices and β-sheets, tubes, etc.) which lack the highly regular ordering and surface area that are thought to play a role in the epitaxial organization of seed nuclei (e.g., [52]). In this respect, most cellular materials are more like the surface of PET bottles than crystals, although there is evidence suggesting that some organisms have evolved mechanisms to control this [5]. In higher animals and plants, most of the nutrients and water are absorbed at the molecular scale via transport processes through cell membranes after digestion; this process tends to exclude the mineral dusts that might be present in an organism's food and water supply.

An exception to this is the presence of occasional biomineral products in animal and plant tissues, which might serve as the ice nucleation sites that normally prevent supercooling. Lowenstam and Weiner [31] reviewed ~60 discrete minerals products that organisms are known to make through biochemical processes, most of which have very specialized roles in the highly-localized formation of bones, teeth, spicules, otoliths, and shells. Lowenstam [30] noted that biominerals range in a spectrum, from minerals that form as an extracellular byproduct 'induced' by biological activity, to highly controlled intracellular precipitates, mediated by specific organic matrices and vesicles. They also range in structural ordering from cryptocrystalline materials like the ball of iron oxide (ferrihydrite) at the core of the ferritin molecule, to the ordered arrays of aragonite needles in the nacre of molluscan shells. Very few of these highly crystalline biomineral products are present in tissues outside the heavily-mineralized areas.

In contrast, nanocrystals of biological magnetite (Fe_3O_4), and its topotactic solid-solution end-member, maghemite, (γ-Fe_2O_3), are broadly distributed at low concentration density throughout many animal tissues, and even in at least one group of plants. Magnetite biomineralization was first discovered in 1962 by Heinz Lowenstam [29] in the teeth of the chitons (marine mollusks of the class *Polyplacophora*), where it hardens the major lateral teeth that the animals use for scraping endolithic algae off of rocky substrates. It was subsequently discovered in the magnetotactic bacteria [12], honeybees [14], homing pigeons [45], fish [46], and even grasses [13]. Although experiments with pulse-remagnetization demonstrate that some of these particles are involved in the ability of animals to detect the geomagnetic field [15,37,50], only a few magnetite-containing cells in an animal would be needed for magnetoreception. Far too much is present in most animal tissues for that to be the only function [17,18].

Specialized studies in the field of rock magnetism using ultrasensitive superconducting quantum-interference device magnetometers (SQUIDS) in clean-lab environments can detect *pico*gram quantities of single-domain magnetite in gram-size tissue samples [47]. Standard rock-magnetic techniques demonstrate that most of these particles are dispersed in isolated particles or small clumps [8,9,19,23], rather than in the concentrated aggregates like the chiton teeth [21]. Typical concentrations of magnetite in animal tissues inferred from these studies range from 1 to 100 ng/g, with particle sizes in the 10–100 nm size range where they have been extracted and examined with high-resolution TEM [19,25,33]. Note that if magnetite crystals in this size range can serve as ice crystal nucleation templates, concentrations as low as 1 ppb can still be significant, as a single 50 nm particle of magnetite in a 50 μm cubic cell occupies 1 ppb by volume. An ice crystal blade nucleating anywhere in a cell at the freezing point could grow large enough to freeze the cell, possibly rupturing the cell membrane. Note that trace concentrations of biogenic magnetite are common in organic matter, potentially confounding the assumption that organic matter is amorphous (e.g., [41]).

It is therefore of fundamental importance for cryobiology and cryopreservation to know whether or not nanocrystals of magnetite like those distributed through many animal and plant tissues are effective for heterogeneous ice crystal nucleation, and whether or not the supercooling process itself has a volumetric effect on the ice expansion process. Similarly, as magnetite is common in the environment, it could play an important role for controlling ice nucleation in nature. It might also serve as an effective ice-nucleating agent in industrial processes where supercooling needs to be inhibited. Hence, we have conducted a series of controlled freezing experiments with well-characterized water samples, with and without added nanophase magnetite, aimed at testing both the nucleation hypothesis, and the concept that ice resulting from supercooled water might have different volume expansion characteristics. Our results support both hypotheses at very highly significant levels, and support the concept that oscillating magnetic fields jiggling ferromagnetic particles in biological samples can explain the reduction of tissue damage during freezing [22].

2. Methods

2.1. Refrigeration system

In order to produce a uniform environment for monitoring the freezing properties of our water samples, we needed a large volume refrigerator that could be controlled accurately and stably in the −20° to 0° temperature range. Our initial measurements of commercial (home) freezers revealed that the cooling cycles were highly variable, particularly those that employed 'defrosting' techniques. We finally converged on the use of a standard −80 °C biological laboratory refrigerator (Nihon freezer CLN-35C), but discovered that the cryogenic design is specifically engineered for the lowest value, with no options of intermediate control. For that reason we created a stable, adjustable-temperature chamber within this using a 50 × 37 × 38 cm Styrofoam™ box with 3 cm thick walls, as shown in Fig. 2. Five of the inside surfaces of the box (all but the top, which had to be removable) were covered with thermal heating pads controlled by an external, tunable proportional–integral–derivative (PID) controller (Omega™ CN76000). To reduce temperature variability within the chamber, we put 0.3 mm thick copper foil over the heating pads, and suspended a small fan on a removable platform over the top to prevent thermal stratification of the cold air in the chamber.

2.2. Standard freezing sphere

To minimize the variability in our experimental results, and to mimic the freezing of typical 100+ gram biological samples, we designed standard balloons made out of stretchable, ~0.1 mm thick polyurethane film (Takeda Sangyou Co., Tokyo) that we could clean in concentrated HCl to remove surface contaminants that are typically present on virtually all laboratory surfaces [24]. Balloons were formed from pairs of 9 cm discs of the film, with 1.5 cm necks, heat-fused along the edges, including the neck. This design allows ~140 g of water without air bubbles to be inserted via an acid-cleaned, 200 ml syringe. (Particles at the air/water interface can sometimes increase ice crystal nucleation [41], so it is important to minimize air bubbles in the experimental balloons.) An example of this balloon is shown in Fig. 2B.

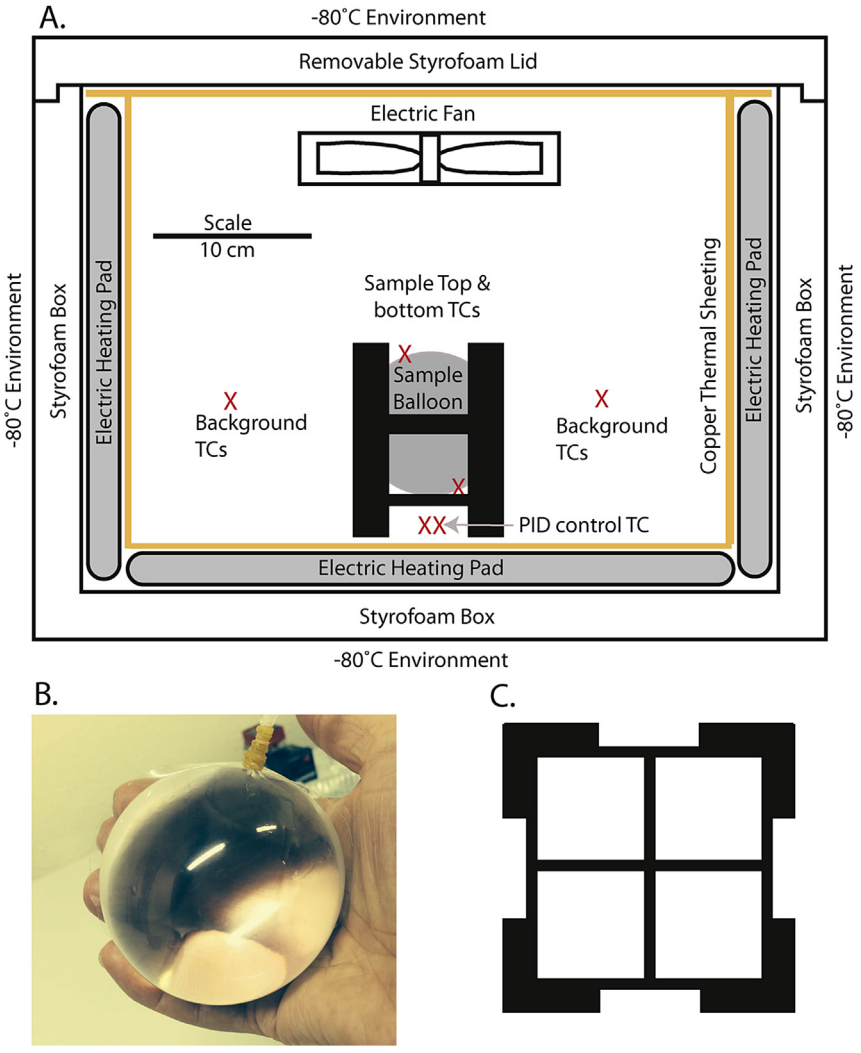

Fig. 2. Thermal monitoring device for standard balloon samples. A. Side-view schematic diagram of the Styrofoam™ experimental freezing chamber, showing the approximate locations of the electric heating pads, the copper sheets, air circulation fan, and the plastic support frame for the balloon samples. As noted in the text, this was placed within a −80 °C laboratory deep-freezer. B. Image of the custom-made polyurethane balloon, filled with water. C. Top-view of the plastic support frame for the standard balloons.

2.3. Water samples

Our ultrapure water samples came from a Yamato Scientific Co., Ltd., WA203 ion exchange/distillation unit. Comparisons reported below were made with the ultra-pure water that had been spiked with a well-characterized magnetite powder, as well as ordinary tap water at the Tokyo Institute of Technology.

2.4. Measurement of volume change

To measure the volume change of these water-filled balloons before and after freezing, we modified a glass flask with a drip nozzle that allowed accurate collection of liquid equal in volume to that of an inserted object. First we poured ethanol chilled to ~ −15 °C to the glass nozzle, then we lowered a water-filled balloon into the container until the top surface was submerged. Then we measured the volume of spilled ethanol, which is the same as that of the balloon before freezing. After the experiment we repeated this measurement on the frozen balloon to measure its volume after freezing. We subtracted the difference and estimated the volume change, as shown in Table 1 and Fig. 3.

2.5. Temperature monitoring circuit

Water-filled balloons described above were inserted into a custom-built plastic support cube that allowed air to circulate freely. Two surface-mounted type “T” thermocouples were taped near the top and bottom of the spherical balloons, with a small quantity of petroleum jelly to ensure good thermal contact. Additional thermocouples were spaced around the freezing container to monitor the temperature within the system. We used a Measurement Computing™ interface board (USB-TC) that allows 8 thermocouples to be monitored simultaneously. Monitoring software was written in C#, using the device drivers provided for this language by the company. Data were recorded in 1 or 2-s intervals, and saved in digital form during the course of all freezing experiments.

2.6. Magnetite powder and dispersion

We used synthetic magnetite power from Toda, Inc., Tokyo, Japan, which has a nominal particle size of 50–100 nm, which we had previously characterized by rock-magnetic properties, and EM [25]. These particles are single magnetic domains that are stably and uniformly magnetized at the saturation value of 92 Am^2/Kg

Table 1
Volume and supercooling data for experimental water samples used in these experiments, as well as results from the t-test of means.

Date of expt.	Volume			Supercooling data	
	Before (ml)	After (ml)	Change (%)	Freezing time (hr)	Supercool temp (°C)
Purified water trials:					
05/01/2015	140	150	7.1	2.21	−12.30
05/12/2015	140	150	7.1	1.57	−11.30
05/14/2015	141	152	7.8	1.58	−11.00
05/19/2015	140	151	7.9	1.35	−11.36
05/21/2015	155	168	8.4	2.21	−12.55
05/26/2015	153	163	6.5	3.17	−12.80
05/28/2015	153	162	5.9	2.42	−12.70
06/29/2015	152	161	5.9	1.94	−12.99
07/03/2015	152	160	5.3	2.77	−13.16
	N = 9	**Mean:**	**6.9**	**2.14**	**−12.24**
		S.D.:	**1.1**	**0.60**	**0.81**
Purified water + Magnetite trials:					
04/30/2015	133	144	8.3	0.28	−2.20
05/11/2015	140	152	8.6	0.15	−2.40
05/13/2015	142	152	7.0	0.13	−4.10
07/02/2015	142	152	7.0	0.57	−8.65
07/06/2015	162	178	9.9	0.71	−1.96
07/08/2015	147	161	9.5	1.03	−2.41
07/09/2015	148	168	13.5	0.23	−1.30
07/16/2015	154	172	11.7	0.65	−1.10
07/18/2015	144	159	10.4	0.68	−2.26
	N = 9	**Mean:**	**9.5**	**0.49**	**−2.93**
		S.D.:	**2.1**	**0.31**	**2.31**
Tap water trials (not used in statistics):					
05/16/2015	140	155	10.7	0.14	−0.70
05/18/2015	140	155	10.7	0.17	−1.00
06/17/2015	131	152	16.0	0.06	−0.20
07/01/2015	138	154	11.6	0.06	−0.23
	N = 4	**Mean:**	**12.3**	**0.11**	**−0.53**
		S.D.:	**2.5**	**0.06**	**0.39**

t-tests of means: Purified water vs. Magnetite-spiked purified water

	d.f.	t-value	2-tailed P-value	Significance
Volume difference:	16	3.36	5.79E-03	**
Time to freezing:	16	7.34	9.00E-06	****
Lowest Supercooling Temp.:	16	11.43	4.90E-07	****

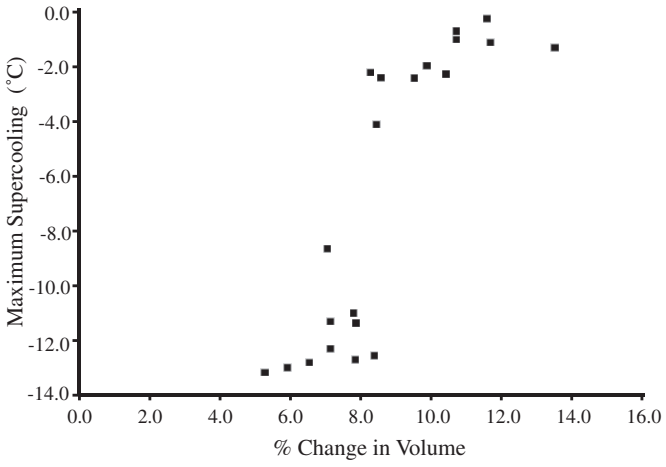

Fig. 3. Relationship between the measured volume change in the standardized polyurethane balloons and the minimum supercooling temperature reached in each experiment (data from Table 1). Note that all visible bubbles were removed from the water samples when the balloons were filled, but that any air bubbles formed during the freezing process will contribute to the measured values.

[3,7]. As these highly magnetic crystals will clump together into dense clusters (e.g., [23]), it is not easy to disperse them into a larger volume of water. Ultrasonic treatment, for example, actually causes particles to 'find' each other and clump together [23]. However, application of an oscillating magnetic field stronger than the microscopic coercivity of the particles can break up these clumps into small strings as the magnetic moments flip, occasionally yielding inter-particle repulsive forces that help to disperse them. Hence, we prepared several liters of magnetite-spiked water by first adding 0.25 ml of the Toda magnetite powder to 0.5 ml of ultrapure water, and then exposing it to a 100 mT, 50 Hz alternating magnetic field using techniques standard in the field of paleomagnetics (e.g. 'Alternating-field demagnetization', see, [2,20]). This was then added to a 500 ml bottle of the water, shaken vigorously, run through additional cycles of alternating-field demagnetization, and the residual (un-dispersed) particles allowed to settle to the bottom. The supernatant liquid, now 'spiked' with ppb-levels of dispersed magnetite, was then further diluted to a volume of several liters for the balloon freezing experiments.

2.7. SQUID magnetometry

To quantify the amount of ferromagnetic material in our water samples (pure, spiked, and tap), we used the class 1000 clean-lab facilities at the California Institute of Technology Paleomagnetics and Biomagnetics laboratories. We modified the standard techniques for assessing the ferromagnetic particles within various type of water (e.g., [4,18,23]), with sensitivity limits down to the picogram/gram range. All sample manipulations and experiments were done in the HEPA-filtered air in the laboratory, including the

sample access chamber of the superconducting moment magnetometer (2G Enterprises™ Model 760 SRM, in a vertical orientation). All glassware was soaked in concentrated HCl to solubilize and remove ferromagnetic contaminants. Approximately 8 g of each liquid was transferred into custom quartz-glass cups, into the center of which we positioned the tip of a ~20 cm long, 3 mm quartz-glass NMR tube. To prevent magnetic particles from physically rotating relative to each other (and hence reducing their net magnetic moment gained after exposure to external magnetic fields), the cup assemblies were then positioned on a cryogenic plate and allowed to freeze solid. Prior to measurement on the superconducting moment magnetometers, the glass was removed by gentle warming, leaving the ~8 g of ice frozen on the end of the glass holder. A complete series of rock-magnetic analyses were then performed at sub-freezing temperatures in a HEPA-filtered nitrogen atmosphere within the superconducting moment magnetometers, as described elsewhere [20,23]. In particular, coercivity spectra were measured via the acquisition and alternating-field (Af) demagnetization of the isothermal remnant magnetism (IRM), and inter-grain interaction effects were measured using acquisition of anhysteretic remanent magnetism (ARM), as well as on the blank quartz-glass holder for assessing signal to noise (see Refs. [4] and [23] for more details). Measured concentrations, based on saturation magnetic remananece values (half that of the full saturation values) are reported in Table 2.

2.8. Data quantification and statistical analysis

Our experiments were designed to test the effect of nanophase magnetite on both the volume change during freezing, and the degree of supercooling, as compared with control samples of purified water. These are actually separate questions, which can be analyzed independently. We ran 9 trials of both groups, as shown in Table 1. The quantitative measure of volume change was computed as a percentage, taken directly from before and after freezing as mentioned above. For the supercooling there were two obvious, and easily-quantified parameters: (1) the time taken from when the balloon first crossed the freezing point (0 °C) until the temperature spike from crystallization appeared, and (2) the lowest temperature reached before that spike (These are shown schematically in Fig. 1A.). Following the recommendation of Saville [40], the null hypothesis of no effect is tested easily with Students' t-test of means for unpaired samples with unequal variance (heteroscedastic), using two-tailed tests. The independence of the volumetric and thermal analyses, and the overall simplicity, argues that a more complex ANOVA is not needed [40]. We did not perform statistical comparisons with the tap water samples, as the materials in it are uncharacterized (except for the magnetization); results are shown here for the sake of qualitative comparison.

3. Results

3.1. Supercooling experiments

Table 1 and Fig. 1 show results from the freezing experiments. The transition from supercooled to the partially frozen state was easily discerned by the abrupt rise in temperature due to the latent heat of crystallization of ice, which quickly brought the entire sphere up to the freezing point.

3.2. SQUID magnetometry

Table 2 shows results from the superconducting magnetometry done to assess the background levels of ferromagnetic materials present in the samples. Magnetization levels of frozen cubes of the purified water samples are only slightly above background noise of the instrument system using the acid-washed quartz glass holder, whereas the purified water with the addition of magnetite, as well as the Tokyo tap water, both had easily detectable levels of ferromagnetic particles. The concentration of magnetite in the 'spiked' water used in our freezing experiments was about 70 ppb, whereas the tap water was about 2 ppb. However, magnetic interaction data (Cisowski's [4] "R" value, and ARM/IRM susceptibility) indicate that the ferromagnetic particles in the tap water are more finely dispersed than those in the magnetite-spiked ultrapure water.

All experiments with purified water run in the polyurethane balloons exhibited clear and obvious supercooling, taking an average of about two hours after crossing the freezing point to reach temperatures between about −11 and −13 °C; this is illustrated in Fig. 1A. In contrast, the purified water to which tiny concentrations of nanophase magnetite crystals had been added displayed far less supercooling, with average temperatures reaching only about −3 °C. Both the measured time, and the minimum temperature reached, before the onset of freezing were shorter, or higher, in comparison with the purified water samples (both P-values are <<0.0001). Hence, we can state with very high confidence that nanophase magnetite comparable to that found in many biological tissues provide effective ice crystal nucleation sites.

Table 1 also shows results of four trials we ran with the tap water. These results are remarkably consistent in terms of their lack of supercooling, with very short time intervals between reaching 0 °C and the onset of the stable freezing regime.

3.3. Ice volume effects

Surprisingly, we also found that the balloons with purified water did not expand as much upon freezing as did those that were spiked with magnetite, or even the tap water; these data are shown in Table 1 and Fig. 3. Our measured volumetric changes were between about 6 and 8% for the supercooled group, compared with 7–13% for the magnetite-spiked group; this difference is highly significant at the $P < 0.01$ level as shown on Table 1. Qualitatively, we noticed that supercooled, pure-water balloons maintained more spherical shapes than those that did not supercool.

4. Discussion

4.1. Overview

Results shown here clearly support the hypothesis that

Table 2
Results of SQUID moment magnetometry for water samples.

Sample	Mass (g)	Saturation moment (Am2)	Magnetization (Am2/Kg)	Cisowski's R-value	ARM/IRM Suscept.	M.D.F. for IRM (mT)	SD Magnetite equivalent (ng/g)
Purified Water	8.04	9.80E-11	1.22E-08	0.39	0.08	39.8	0.3
Purified Water + Magnetite	8.12	2.54E-08	3.13E-06	0.27	0.01	17.4	68.1
Tap water	7.92	7.64E-10	9.65E-08	0.40	0.10	37.1	2.1

nanocrystals of magnetite act as effective ice crystal nucleation particles. To our knowledge this is the first experimental test of this effect on this mineral, which is one of the most widely-dispersed mineral products in the biosphere, as well as being common trace mineral in the natural environment. Nucleation temperatures that we observed in the presence of magnetite are high in comparison with other cryopreservation systems, which typically supercool to much colder temperatures, e.g Ref. [36]. We also observed a surprising association between the degree of supercooling and an apparent volume change, which may have implications for cryobiology and cryopreservation.

4.2. Volume changes

Our observation that the balloon volume varies sharply for those that supercooled to <4 °C (shown on Fig. 3) was unexpected, and surprising. Our balloons that supercooled also displayed fewer elongate ice crystals deforming their shape. Upon closer examination, it seems that ice formed without supercooling may be degassing more, as our impression was that small bubbles were found more often within those balloons than for those that had supercooled; and the presence of bubbles within the balloons would obviously have a significant effect on our volume measurement. It might be that supercooling to < −4 °C promotes the entrapment of dissolved gasses in a clathrate-like form, and might also promote the formation of the structurally-disordered ice polymorph (I_{sd}), instead of the usual hexagonal form (I_h), as argued by Malkin et al. [32]. However, they did not comment on volumetric differences between the two ice states (disordered I_{sd}, and ordered I_h). Nevertheless, a decrease in degassing within a biological cell during freezing would similarly decrease the net volume change, and potentially result in less damage to biological membranes.

4.3. Comparison with previous work

Our experiments were designed to mimic the freezing process of typical biological tissues, which for the human food supply are on the order of a few hundred grams or more in size. However, it is worth comparing our results to kindred experiments that have been done in the atmospheric sciences trying to understand the chemistry and kinetics of heterogeneous ice nucleating particles in supercooled water droplets suspended at high altitudes in clouds. In particular, Atkinson et al. [1] and Whale et al. [49] describe experiments on arrays of hundreds of microliter-sized water droplets, spiked with suspensions of powdered minerals at concentrations up to 1%, held on hydrophobic slides and imaged during the cooling process. They concluded that the potassium feldspars minerals were most effective of all of the common dust minerals they examined in the heterogeneous nucleation of ice in supercooled droplets (although they did not test magnetite). (We note that nanophase magnetite also commonly exsolves in silicates, and might confound freezing experiments with other minerals [10,11,43,44]). In contrast, our 'drops' were ~140 cc balloons, spiked with ~70 ng/g of standard magnetite powder designed to mimic levels in biological tissues. Due to the much finer grain size or our magnetite, our samples contain roughly the same active surface area per experiment as did their studies (within an order of magnitude; see tab #4 of the supplemental spreadsheet), and our technique allows easy measurement of volume changes. Comparing the fraction of balloons frozen as temperature falls, to the micro-drop data on Fig. 1a of Atkinson et al. [1] gives a dramatic comparison: the average temperature of magnetite-spiked freezing is about −3 °C, compared with −22 °C for solutions of up to 1% K-feldspar. Unfortunately, it is not clear that the microdrop experiments would work well on dense dispersions of magnetite nanoparticles, as the tiny crystals will stick together and drop out of suspension. Nevertheless, it seems that magnetite nucleates ice more efficiently than K-feldspar.

4.4. Applications

Magnetite nano-crystalline powders, if properly dispersed, might also serve as a simple and effective ice-nucleating agent in a variety of freezing process in which supercooling needs to be avoided. Cochet and Widehem [5] review several of these in the context of using the bacterium, *Pseudomonas syringae*, to enhance the procedures. These include the preparation of frozen food (wherein supercooling increases the energy cost of freezing), freeze-concentration processes, and spray-ice technology (e.g., snow-making). However, in food application processes the use of magnetite would not require the containment or sterilization processes that are required when using biologically active cells.

5. Conclusion, and relevance to the magnetically-assisted freezing controversy

Two factors have been discussed extensively in the Cryobiology literature that together seem to influence the viability of tissues and cells during cryopreservation. These include the intracellular formation of ice crystals that can damage and rupture cell membranes, and the change in osmotic and concentration gradients acting between the inside and exteriors of cells during freezing [34]. These factors account for the peak survivability of many tissue types at intermediate cooling rates, and as well as differential revival abilities during subsequent warming stages. However, reasons for the success of various cryopreservation techniques in some organisms, and their dismal failure in related species (e.g., monkeys vs. humans) have been mystifying [34]. We note here that biological magnetite concentrations are also highly variable between tissue types within a given species, and between many animal groups (see Ref. [18]). In addition, magnetite is often present as environmental contaminants at variable trace levels in many growth media used to main cell lines in culture [24]. Coupled with the observation reported here that magnetite is an effective ice-crystal nucleating material, it may help resolve some of this variability in cryopreservation. New analytical techniques such as scanning SQUID microscopy [48] and quantum-diamond magnetic imaging [26] are capable of detecting single crystals of biological magnetite within cells, and could potentially test this hypothesis.

Finally, we note that magnetite is a ferromagnetic (more specifically, ferrimagnetic) material. We suggested recently [22] that the apparent action of weak, ~10 Hz, ~1 mT oscillating magnetic fields to minimize ice crystal damage in plant and animal tissues during freezing [16,27,28,38,39] might be explained simply by the induced, magneto-mechanical motion of these nanoparticles of magnetite disturbing incipient nucleation sites on the magnetite crystal surfaces, promoting local supercooling. This hypothesis side-steps many of the biophysical critiques that have been leveled against this "Cells Alive System" [42,51]. In terms of Cryobiology, our experiments indicate that the trace amounts of magnetite that are present in many biological tissues ought to nucleate at least some fraction of the ice crystals that cause tissue damage during freezing. Two observations suggest that the sudden crystallization of such supercooled water might minimize cellular damage, including the lower volumetric expansion noted on Fig. 3, and the tendency of supercooled water to generate the structurally-disordered ice polymorph (I_{sd}), which does not form needle-like crystals like the more slowly-grown hexagonal ice, I_h [32]. As noted above, a single 50 nm particle of magnetite suspended in a 50 μm cell would occupy a volume fraction of 1 ppb; many animal

and plant tissues have finely-distributed magnetite crystals at levels that are well above this. It is intriguing that externally-oscillating magnetic fields acting on magnetite crystals might allow the nucleating process to be switched on or off during the freezing process, allowing greater control of the resulting ice crystal size and morphology. Further experimental tests of this hypothesis are in progress.

Acknowledgments

This study was supported by: (1) JSPS KAKENHI Grant Number JP26630062 from the Japan Society for the Promotion of Science, in the category "Challenging Exploratory Research 2014" to AK and HNG, (2) discretionary funds from Caltech to JLK; funding agencies did not influence the results of this work, and the authors have no conflict of interests. We thank Prof. Hideo Tsunakawa of the Tokyo Institute of Technology for the use of the Alternating-field demagnetization unit.

Appendix A. Supplementary data

Supplementary data related to this article can be found at http://dx.doi.org/10.1016/j.cryobiol.2016.04.003.

References

[1] J.D. Atkinson, B.J. Murray, M.T. Woodhouse, T.F. Whale, K.J. Baustian, K.S. Carslaw, S. Dobbie, D. O'Sullivan, T.L. Malkin, The importance of feldspar for ice nucleation by mineral dust in mixed-phase clouds, Nature 498 (2013) 355–358.
[2] R.F. Butler, Paleomagnetism: Magnetic Domains to Geologic Terranes, Blackwell Scientific Publications, Boston, 1992.
[3] R.F. Butler, S.K. Banerjee, Theoretical single-domain size range in magnetite and titanomagnetite, J. Geophys. Res. 80 (1975) 4049–4058.
[4] S. Cisowski, Interacting vs. non-interacting single-domain behavior in natural and synthetic samples, Phys. Earth Planet. Inter. 26 (1981) 56–62.
[5] N. Cochet, P. Widehem, Ice crystallization by pseudomonas syringae, Appl. Microbiol. Biot. 54 (2000) 153–161.
[6] R. Dahl, L.A. Staehelin, High-pressure freezing for the preservatino of biological structure - theory and practice, J. Electron Microsc. Tech. 13 (1989) 165–174.
[7] J.C. Diaz Ricci, J.L. Kirschvink, Magnetic domain state and coercivity predictions for biogenic greigite (Fe_3S_4): a comparison of theory with magnetosome observations, J. Geophys. Res. 97 (1992) 17309–17315.
[8] J. Dobson, P. Grass, Magnetic properties of human hippocampal tissue – evaluation of artefact and contamination sources, Brain Res. Bull. 39 (1996) 255–259.
[9] J.R. Dunn, M. Fuller, J. Zoeger, J. Dobson, F. Heller, J. Hammann, E. Caine, B.M. Moskowitz, Magnetic material in the human hippocampus, Brain Res. Bull. 36 (1995) 149–153.
[10] J.M. Feinberg, R.J. Harrison, T. Kasama, R.E. Dunin-Borkowski, G.R. Scott, P.R. Renne, Effects of internal mineral structures on the magnetic remanence of silicate-hosted titanomagnetite inclusions: an electron holography study, J. Geophys. Res. Solid Earth 111 (2006).
[11] J.M. Feinberg, G.R. Scott, P.R. Renne, H.R. Wenk, Exsolved magnetite inclusions in silicates: features determining their remanence behavior, Geology 33 (2005) 513–516.
[12] R.B. Frankel, R.P. Blakemore, R.S. Wolfe, Magnetite in freshwater magnetotactic bacteria, Science 203 (1979) 1355–1356.
[13] M. Gajdardziska-Josifovska, R.G. McClean, M.A. Schofield, C.V. Sommer, W.F. Kean, Discovery of nanocrystalline botanical magnetite, Eur. J. Mineral. 13 (2001) 863–870.
[14] J.L. Gould, J.L. Kirschvink, K.S. Deffeyes, Bees have magnetic remanence, Science 201 (1978) 1026–1028.
[15] R.A. Holland, J.L. Kirschvink, T.G. Doak, M. Wikelski, Bats use magnetite to detect the Earth's magnetic field, Plos One 3 (2008) e1676–6.
[16] M. Kaku, T. Kawata, S. Abedini, H. Koseki, S. Kojima, H. Sumi, H. Shikata, M. Motokawa, T. Fujita, J. Ohtani, N. Ohwada, M. Kurita, K. Tanne, Electric and magnetic fields in cryopreservation: a response, Cryobiology 64 (2012) 304–305.
[17] J.L. Kirschvink, Rock magnetism linked to human brain magnetite, EOS Trans. Am. Geophys. Union 75 (1994) 178–179.
[18] J.L. Kirschvink, D.S. Jones, B.J. McFadden, Magnetite Biomineralization and Magnetoreception in Organisms: a New Biomagnetism, Plenum Press, New York, N.Y, 1985.
[19] J.L. Kirschvink, A. Kobayashi, B.J. Woodford, Magnetite biomineralization in the human brain, Proc. Natl. Acad. Sci. 89 (1992) 7683–7687.
[20] J.L. Kirschvink, R.E. Kopp, T.D. Raub, C.T. Baumgartner, J.W. Holt, Rapid, precise, and high-sensitivity acquisition of paleomagnetic and rock-magnetic data: development of a low-noise automatic sample changing system for superconducting rock magnetometers, Geochem. Geophys. Geosyst. 9 (2008) 1–18.
[21] J.L. Kirschvink, H.A. Lowenstam, Mineralization and magnetization of chiton teeth: paleomagnetic, sedimentologic, and biologic implications of organic magnetite, Earth Planet. Sci. Lett. 44 (1979) 193–204.
[22] A. Kobayashi, J.L. Kirschvink, A ferromagnetic model for the action of electric and magnetic fields in cryopreservation, Cryobiology 68 (2014) 163–165.
[23] A. Kobayashi, J.L. Kirschvink, C.Z. Nash, R.E. Kopp, D.A. Sauer, L.E. Bertani, W.F. Voorhout, T. Taguchi, Experimental observation of magnetosome chain collapse in magnetotactic bacteria: sedimentological, paleomagnetic, and evolutionary implications, Earth Planet. Sci. Lett. 245 (2006) 538–550.
[24] A. Kobayashi, J.L. Kirschvink, M.H. Nesson, Ferromagnets and EMFs, Nature 374 (1995), 123–123.
[25] A. Kobayashi, N. Yamamoto, J.L. Kirschvink, Studies of inorganic crystals in biological tissue – magnetite in human tumor, J. Jpn. Soc. Powder Powder Metall. 44 (1997) 294–300.
[26] D. Le Sage, K. Arai, D.R. Glenn, S.J. DeVience, L.M. Pham, L. Rahn-Lee, M.D. Lukin, A. Yacoby, A. Komeili, R.L. Walsworth, Optical magnetic imaging of living cells, Nature 496 (2013), 486–U105.
[27] S.Y. Lee, G.W. Huang, J.N. Shiung, Y.H. Huang, J.H. Jeng, T.F. Kuo, J.C. Yang, W.C.V. Yang, Magnetic cryopreservation for dental pulp stem cells, Cells Tissues Organs 196 (2012) 23–33.
[28] P.Y. Lin, Y.C. Yang, S.H. Hung, S.Y. Lee, M.S. Lee, M. Chu, S.M. Hwang, Cryopreservation of human embryonic stem cells by a programmed freezer with an oscillating magnetic field, Cryobiology 66 (2013) 256–260.
[29] H.A. Lowenstam, Magnetite in denticle capping in recent chitons (*polyplacophora*), Geol. Soc. Am. Bull. 73 (1962) 435–438.
[30] H.A. Lowenstam, Minerals made by organisms, Science 211 (1981) 1126–1131.
[31] H.A. Lowenstam, S. Weiner, On Biomineralization, Oxford University Press, Oxford, 1989.
[32] T.L. Malkin, B.J. Murray, C.G. Salzmann, V. Molinero, S.J. Pickering, T.F. Whale, Stacking disorder in ice I, Phys. Chem. Chem. Phys. 17 (2015) 60–76.
[33] S. Mann, N.H.C. Sparks, M.M. Walker, J.L. Kirschvink, Ultrastructure, morphology and organization of biogenic magnetite from sockeye salmon, *Oncorhynchus nerka*: implications for magnetoreception, J. Exp. Biol. 140 (1988) 35–49.
[34] P. Mazur, S.P. Leibo, G.E. Seidel, Cryopreservation of the germplasm of animals used in biological and medical research: importance, impact, status, and future directions, Biol. Reprod. 78 (2008) 2–12.
[35] E.B. Moore, V. Molinero, Structural transformation in supercooled water controls the crystallization rate of ice, Nature 479 (2011), 506–U226.
[36] G.J. Morris, E. Acton, Controlled ice nucleation in cryopreservation – a review, Cryobiology 66 (2013) 85–92.
[37] U. Munro, J.A. Munro, J.B. Phillips, R. Wiltschko, W. Wiltschko, Evidence for a magnetite-based navigational map in birds, Naturwissenschaften 84 (1997) 26–28.
[38] N. Owada, S. Kurita, in: U.S.p. office (Ed.), Super-quick Freezing Method and Apparatus Therefor, ABI Limited, Chiba, Japan, United States of America, 2001. US 6,250,087 B1.
[39] N. Owada, S. Saito, in: U.S.p. office (Ed.), Quick Freezing Apparatus and Quick Freezing Method, 2010, p. 15. USP 7,810,340 B2, Owada, N., United States of America.
[40] D.J. Saville, Multiple comparison procedures – the practical solution, Am. Stat. 44 (1990) 174–180.
[41] R.A. Shaw, A.J. Durant, Y. Mi, Heterogeneous surface crystallization observed in undercooled water, J. Phys. Chem. B 109 (2005) 9865–9868.
[42] T. Suzuki, Y. Takeuchi, K. Masuda, M. Watanabe, R. Shirakashi, Y. Fukuda, T. Tsuruta, K. Yamamoto, N. Koga, N. Hiruma, J. Ichioka, K. Takail, Experimental investigation of effectiveness of magnetic field on food freezing process, Trans. Jpn. Soc. Refrig. Air Cond. Eng. 26 (2009) 371–386.
[43] J.A. Tarduno, R.D. Cottrell, A.V. Smirnov, High geomagnetic intensity during the mid-cretaceous from Thellier analyses of single plagioclase crystals, Science 291 (2001) 1779–1783.
[44] J.A. Tarduno, R.D. Cottrell, M.K. Watkeys, D. Bauch, Geomagnetic field strength 3.2 billion years ago recorded by single silicate crystals, Nature 446 (2007) 657–660.
[45] C. Walcott, J.L. Gould, J.L. Kirschvink, Pigeons have magnets, Science 205 (1979) 1027–1029.
[46] M.M. Walker, J.L. Kirschvink, S.-B.R. Chang, A.E. Dizon, A candidate magnetic sense organ in the Yellowfin Tuna Thunnus albacares, Science 224 (1984) 751–753.
[47] M.M. Walker, J.L. Kirschvink, A.S. Perry, A.E. Dizon, Methods and techniques for the detection, extraction, and characterization of biogenic magnetite, in: J.L. Kirschvink, D.S. Jones, B.J. McFadden (Eds.), Magnetite Biomineralization and Magnetoreception in Organisms: a New Biomagnetism, Plenum Press, New York, 1985, pp. 154–166.
[48] B.P. Weiss, F.J. Baudenbacher, J.P. Wikswo, J.L. Kirschvink, Magnetic microscopy promises a leap in sensitivity and resolution, Eos Trans. AGU 82 (2001) 513–518.
[49] T.F. Whale, B.J. Murray, D. O'Sullivan, T.W. Wilson, N.S. Umo, K.J. Baustian, J.D. Atkinson, D.A. Workneh, G.J. Morris, A technique for quantifying

heterogeneous ice nucleation in microlitre supercooled water droplets, Atmos. Meas. Tech. 8 (2015) 2437–2447.
[50] W. Wiltschko, U. Munro, R.C. Beason, H. Ford, R. Wiltschko, A magnetic pulse leads to a temporary deflection in the orientation of migratory birds, Experimentia 50 (1994) 697–700.
[51] B. Wowk, Electric and magnetic fields in cryopreservation, Cryobiology 64 (2012) 301–303.
[52] X.X. Zhang, M. Chen, M. Fu, Impact of surface nanostructure on ice nucleation, J. Chem. Phys. 141 (2014).